

Quantitative assessment of mudstone lithology using geophysical wireline logs and artificial neural networks

Yunlai Yang, Andrew C. Aplin and Steve R. Larter

NRG, School of Civil Engineering and Geosciences, University of Newcastle, Newcastle upon Tyne NE1 7RU, UK

ABSTRACT: Using a dataset of 530 analysed mudstone samples from 19 North Sea and 9 Gulf of Mexico wells, back propagation artificial neural networks (ANNs) have been trained to estimate the clay content (proportion of particles smaller than 2 μm diameter), grain density and total organic content (TOC) of mudstones from standard wireline log data (gamma, resistivity, sonic, density, calliper). ANNs have also been trained to discriminate carbonates from clastic mudstones and also give a preliminary indication of the extent to which mudstones are lithified or cemented. Results show that for clay content, 85% of predictions are within $\pm 10\%$ of the measured value; for TOC, 92% of predictions are within $\pm 1\%$ of the measured value; for grain density, 91% of predictions are within $\pm 0.07 \text{ g cm}^{-3}$ of the measured value; for the discrimination of carbonates from clastics, 98.3% of carbonate samples and 99.9% of non-carbonate samples are classified correctly. The ANNs work well not only in the areas from where training data were measured, but also (as an example) in offshore West Africa. Potential applications of the technique include (1) the possibility to define the 3D sedimentary architecture of mudstone sequences from wireline data and, because both the porosity–effective stress and porosity–permeability relationships of mudstones are strongly influenced by clay content, (2) more accurate, basin-scale fluid flow modelling.

KEYWORDS: *mudstone, wireline log, petrophysics, artificial neural network*

INTRODUCTION

Fine-grained clastic sediments are both compositionally diverse and heterogeneous (e.g. Picard 1971). Lithological diversity results in a similarly wide range of physical properties, including geologically important parameters such as compressibility (porosity: effective stress relationships), the relationships between porosity and permeability and the critical capillary entry pressure (Skempton 1970; Borst 1982; Burland 1990; Katsube & Williamson 1994; Neuzil 1994; Aplin *et al.* 1995; Schlömer & Krooss, 1997; Dewhurst *et al.* 1998; 1999*a, b*; Yang & Aplin 1998). From the petroleum geological perspective, these relationships are fundamental to assessments of pore pressure based on mudstone porosity (e.g. Alixant & Desbrandes 1991; Schneider *et al.* 1993; Burrus 1998) and as inputs to computer-based basin modelling (e.g. Smith 1971; Sharp & Domenico 1976; Yukler *et al.* 1978; Bethke 1985; Lerche 1990; Ungerer *et al.* 1990; Luo & Vasseur 1992).

Both the porosity–permeability and porosity–effective stress relationships of mudstones are strongly influenced by lithology, which can be expressed simply but robustly as clay content, the percentage of particles that have a diameter of less than 2 μm (Skempton 1944; Aplin *et al.* 1995; Dewhurst *et al.* 1998; 1999*a, b*; Yang & Aplin 1998). It is also likely, although less well constrained currently, that the critical capillary entry pressure of mudstones is influenced, at a given porosity, by grain size (Kaldi & Atkinson 1997; Dewhurst *et al.* 1998; 1999*a*; Yang & Aplin 1998). Estimation of mudstones' clay content, thus, yields a promising way of constraining the void ratio–effective stress,

permeability–void ratio and porosity–capillary entry pressure relationships which are required for basin modelling and pore pressure evaluation.

Although clay content can be measured in the laboratory (Yang & Aplin 1997), a measurement-centred approach to mudstone properties is unrealistic on a large scale. In this paper, the use of wireline log data to evaluate clay content is explored. Previous workers have used either the gamma ray log or a combination of the neutron and density logs to assess the clay mineral content of mudstones (see Doveton 1994; Hearst *et al.* 2000). The approach outlined here is somewhat different; since the relationship between log response and clay content is quite complex and non-linear, the study employs a suite of logs and uses an artificial neural network (ANN) technique as a modelling tool by which certain physical properties of mudstones, such as clay content and grain density, can be quickly and quantitatively related to the wireline response.

Over the past few years, over 500 samples from 19 North Sea (NS) and 9 Gulf of Mexico (GOM) wells have been systematically characterized in terms of their clay content, grain density, total organic content (TOC), porosity and pore size distribution. This paper describes how these data have been used to construct ANN models that allow lithological parameters such as clay content, grain density and TOC to be estimated from wireline log data.

ARTIFICIAL NEURAL NETWORKS

An artificial neural network is a mathematical model in which a desired output (e.g. clay content) is derived from a complex set

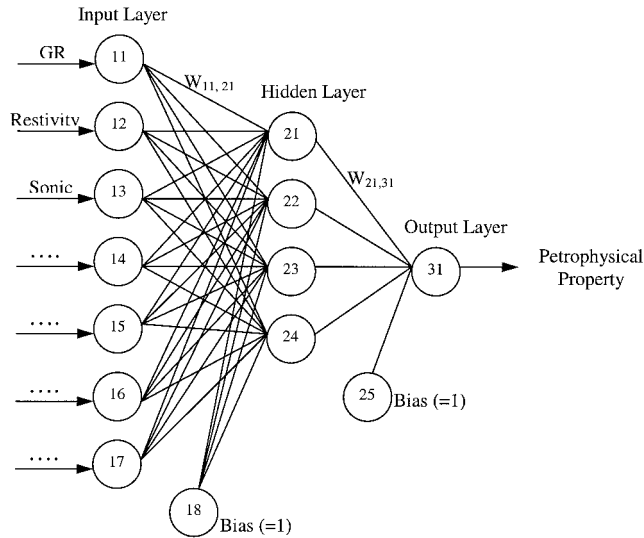


Fig. 1. Architecture of a back propagation artificial neural network.

of input data (e.g. wireline log data). The approach is empirical in that the ANN is first presented with both input data (wireline log data) and output data (for example, laboratory-measured clay content data) and is **trained** to recognize the output data from multiple input data through the derivation of non-linear relationships between the two. Once the network is trained, it can be presented with new data and used to derive new outputs very quickly. Given their ability to locate the kind of complex, non-linear relationships that are common in geological systems, ANNs represent a sensible choice for the quantitative estimation of geologically useful parameters from relatively simple and commonly available input data (see Doveton (1994) for a review). Published examples of the use of ANNs in petroleum geology include the derivation of lithology from wireline logs (Baldwin *et al.* 1990; Rogers *et al.* 1992), the analysis of seismic data (Pulli & Dysart 1990; Wang 1992), source rock characterization (Huang & Williamson 1996), reservoir permeability estimation (Osborne 1992; Rogers *et al.* 1995) and reserves estimation (Wu & Zhou 1992).

Of the various types of available ANN, a back propagation network was chosen for this work. Figure 1 shows a representation of an ANN in which layers of nodes are connected by synapses. There is an input layer (log data in this case), an output layer (rock property data in this case) and a number of hidden layers. The value of the node in the input layer is normally within the range between zero and one, so that in real applications, input values are rescaled to a range between zero and one. In each layer except for the output, there is an additional 'bias' node which is assigned a constant value, usually equal to one (see Zupan & Gasteiger (1993) for more detail). The arithmetic value of any node is equal to the sum of the outputs of the nodes in the preceding layer, each multiplied by the weight of the connecting synapse:

$$Net_{i,j} = \sum_{k=1}^n Out_{i-1,k} \times w_{i-1,k;i,j} \quad (1)$$

where $Net_{i,j}$ is the value of the j th node in layer i , $Out_{i-1,k}$ is the output of the k th node in the preceding layer ($i-1$) and $w_{i-1,k;i,j}$ is the weight of the synapse between node j in layer i and node k in the preceding layer ($i-1$).

The output of a node in the input layer is simply its own value. In contrast, the output of a node in the hidden and output layers is generated by transforming its own value ($Net_{i,j}$) using a transfer function. Most ANNs use sigmoidal transfer functions to model the transfer from its own value to output signals:

$$Out_{i,j} = \frac{1}{1 + \exp(-a \cdot Net_{i,j} + v)} \quad (2)$$

where a and v are positive constants, usually set to 1 and 0. Note that because the value of the sigmoidal transfer function ranges from 0 to 1 and that the output of a network is in the range between 0 and 1, the output must be rescaled to the true value.

In summary, then, each node in a layer (apart from the input layer) receives input from every node in the previous layer and then sums the weighted inputs to give its own value. Its value is then transformed according to a chosen transfer function and the transformed value is then output to every node in the next layer. By transferring information in this way, a network receives a set of input data and transforms it to a set of required output data.

There are three steps in the construction of an ANN model. First, decisions are taken regarding both the architecture (number of hidden layers and number of nodes in each hidden layer) and the transfer function to be used. Second, the numerical weights of synapses are determined by a network training procedure. Third, the ability of the ANN to model new and unseen datasets is tested.

Training involves repeatedly presenting a set of inputs to the ANN and modifying the weights of the synapses in order to derive a sufficiently accurate match with a desired result. In this case, the 'input data' would be a suite of log data and the 'desired result' would be a lithological parameter such as clay content. Using an arbitrary choice of initial weights, the ANN produces output values which are then compared with the desired result, or **pattern**. The patterns are scaled within the range between 0 and 1 before training, since the range of outputs of a network is between 0 and 1. Training is accomplished by the **back-propagation of errors** (difference between output and correct value) through the network, which involves changing the weights of synapses between nodes. The correction to the weight of each synapse is based on the error, the input to the node and the correction of the previous cycle (see Rummelhart & McClelland (1986), Zupan & Gasteiger (1993) and Patterson (1995) for more detail). Weights are changed gradually and converge to an equilibrium setting, at which point the network is said to be **trained**.

Testing of ANNs is critical to an assessment of its ability to work with new datasets. One approach to this is to train the ANN with a certain percentage (e.g. 80%) of the input data and to test the network with the other 20%. Additional datasets are also important for testing the ability of the ANN to work in a wide range of settings.

DATA

Mudstone physical properties

In the study, 530 samples were analysed – 290 from 19 North Sea wells and 240 from 9 Gulf of Mexico wells. The North Sea samples range in age from Quaternary to Jurassic and in depth between 550 m and 4500 m. Most samples are cuttings, with some sidewall cores. The Gulf of Mexico samples are Tertiary

Table 1. Summary of results of network training for carbonate–clastic discrimination

Model type	Data source			Error	
	North Sea (Total/carbonate)	GoM (Total/carbonate)	Total (Total/carbonate)	Carbonate → Mudstone (%)	Mudstone → carbonate (%)
NS–GoM model with density log	510/134	565/107	1075/241	1.7	0.1
NS–GoM model without density log	510/138	538/105	1048/243	2.1	0.4

Error refers to percentage of outputs incorrectly ascribed to carbonate or clastic sediment.

Table 2. Summary of results of network training for grain density, TOC and clay content

Model type	Data source			% of output data with error of value				<i>r</i>
	North Sea	GoM	Total					
Grain density (g cm^{-3})				0.03	0.05	0.07	0.1	
North Sea model	205		205	49	74	91	96	0.75
NS–GoM model with density log	205	225	430	48	74	91	99	0.63
NS–GoM model without density log	224	226	450	47	72	87	98	0.57
TOC (%)				0.5	1	1.5		
North Sea model	209		209	58	85	97		0.92
NS–GoM model with density log	256	236	492	72	92	98		0.89
NS–GoM model without density log	290	236	526	67	92	97		0.87
Clay content (%)				5	7	10	15	
North Sea model	137		137	52	71	86	98	0.903
NS–GoM model with density log	137	237	374	47	69	85	98	0.824
NS–GoM model without density log	161	237	398	49	64	82	95	0.805

r is correlation coefficient.

in age, from burial depths between 1500 m and 5200 m. Most samples are sidewall cores, with some cuttings and conventional core plugs.

The particle size distribution, TOC and grain density were measured on all samples and specific surface area and mineral composition were measured on some. Samples were gently disaggregated using a freeze–thaw technique (Yang & Aplin 1997) prior to particle size measurement. The particle size was measured using either the sedimentation pipette method (British Standard 1377: British Standards 1990) or a Micromeritics Sedigraph 5000ET particle size analyser, which had been calibrated against the standard pipette method. The grain densities were measured by the small pycnometer method (British Standard 1377: British Standards 1990). Specific surface area was measured on intact, dried samples using a Micromeritics Flowsorb 2300 surface area analyser (e.g. Ross & Oliver 1964; Gregg & Sing 1967). Mineralogy was determined semi-quantitatively by X-ray diffraction.

The physical properties that are of interest here and for which the ANNs were trained are:

1. clay content, the mass percentage of particles with a diameter of $<2 \mu\text{m}$;
2. grain density, which is required for the accurate calculation of porosity from the density log;
3. TOC – other techniques have been used to estimate TOC from wireline logs (Schmoker 1979, 1981; Meyer & Nederlof 1984), including the use of ANNs (Huang & Williamson 1996);
4. cementation factor – this is a qualitative parameter which, although it is by no means perfectly constrained, is introduced here because it can give a rapid indication of the extent to which the physical properties of mudstones have been altered by processes such as cementation or lithification. The parameter is based on experience of disaggregating mudstones for the determination of grain size distributions. The procedure is based on a freeze–thaw

method which gently disaggregates the sediment (Yang & Aplin 1997). This technique failed to disaggregate a series of mudstones from a 400 m mudstone unit in one North Sea well. Further analyses indicated that these mudstones were cemented with calcium carbonate and had specific surface areas between $2 \text{ m}^2 \text{ g}^{-1}$ and $5 \text{ m}^2 \text{ g}^{-1}$, compared to values of $15\text{--}60 \text{ m}^2 \text{ g}^{-1}$ for most samples. A parameter is, therefore, proposed – the cementation factor – which varies from 0 (uncemented/unlithified) to 1 (cemented/lithified). For the purposes of training the ANNs, sediments from the cemented mudstone unit of the North Sea well were assigned a cementation factor of 1. Cementation factors of zero were assigned to all other samples that could be easily disaggregated. Log data were averaged over a 1 m interval, resulting in a dataset of around 100 points for cemented samples and around 600 points for uncemented samples.

Since the focus here is on fine-grained clastic sediments, ANNs were also constructed to differentiate fine-grained clastics from carbonates. For this purpose, over 1000 log data points were collected from 1 m intervals in both carbonate and non-carbonate (sand and mudstone) sections from all wells.

Samples represent a wide range of mudstone lithotypes. For the North Sea samples, grain densities range from 2.5 g cm^{-3} to 2.88 g cm^{-3} , TOC between 0.3% and 8.5% and clay content between 13% and 90%. This covers close to the entire spectrum normally encountered in a sedimentary basin. For the Gulf of Mexico samples, the range of clay contents is high (20–73%) but the range of grain density and TOC is narrow, reflecting the lack of a source rock in the drilled sections of the Gulf. The statistics of the datasets used to construct each of the ANN models are listed in Tables 1 and 2.

Wireline logs

Calliper, deep resistivity, gamma ray, sonic transit time and density logs were used as inputs to the ANNs, along with burial

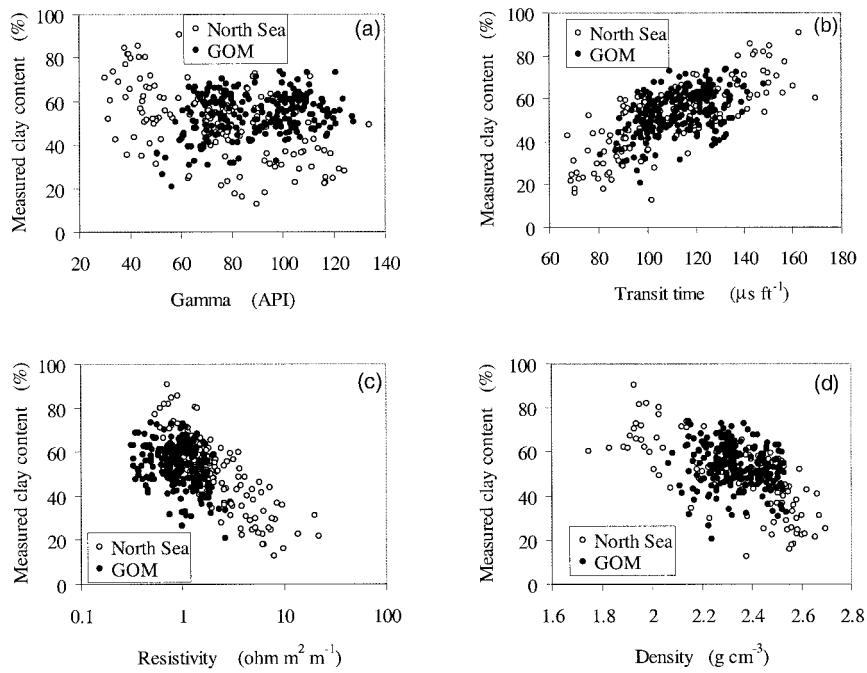


Fig. 2. Correlations between measured clay content and wireline log values of (a) gamma ray; (b) sonic transit time; (c) log resistivity; and (d) density.

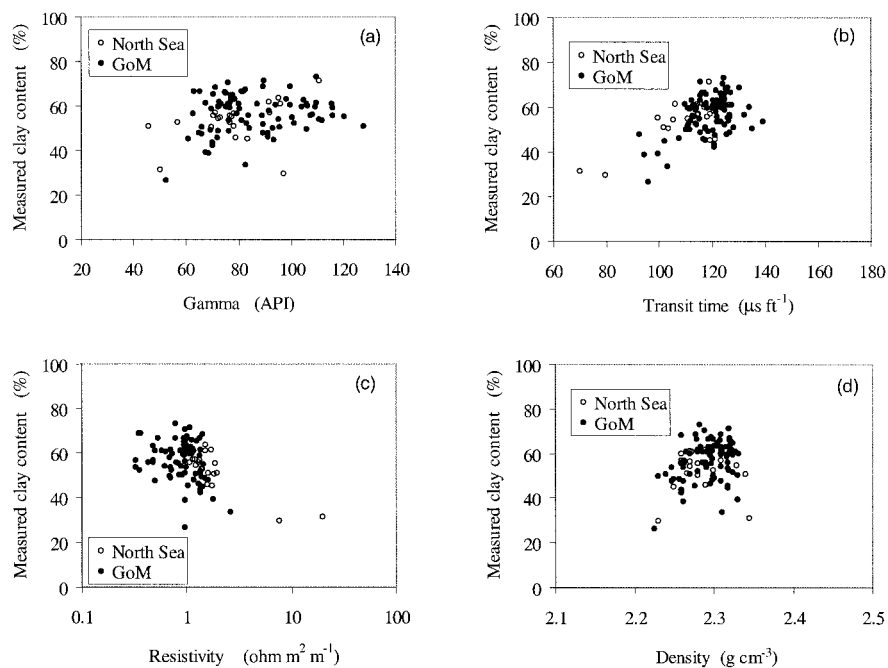


Fig. 3. Correlations between measured clay content and wireline log values of (a) gamma ray; (b) sonic transit time; (c) log resistivity; and (d) density, for samples with porosities between 25% and 30%.

depth and drilling bit size. For cuttings samples, log data were averaged over 3 m depth intervals. For sidewall core and conventional core samples, log data were taken from the specific depth of the core.

It has already been pointed out that one of the strengths of ANNs is their ability to locate complex, non-linear relationships between variables. The need to use a technique such as ANNs as a way of relating wireline data to the petrophysical properties of mudstones is shown in Figures 2 and 3, which show cross-plots of individual wireline responses against clay content. Figure 2 shows the complete dataset and Figure 3 shows the data for samples with similar porosities, between 25% and 30%. Comparison of Figures 2 and 3 indicates that some of the weak correlations between clay content and sonic transit time, resistivity or density are not causative but relate to the nature of

the dataset, in which, by chance, the deeper, lower porosity samples are often more coarse-grained than the shallower, more porous samples. This largely reflects the generally more coarse-grained muds of the shallow marine and deltaic depositional environment of the North Sea Jurassic, compared to the post-Jurassic, deeper-water setting. When the effects of porosity are screened out of the dataset, there is little correlation between clay content and the response of an individual geophysical log (Fig. 3). Should clay content be estimated directly from any one of these logs alone, an unacceptably large error of $\pm 20\%$ will, thus, ensue. One slight surprise is that there is no obvious correlation between gamma ray response and clay content. Most strikingly, most of the lower Tertiary samples from the North Sea wells are very fine grained, with clay contents between 70% and 85%. The samples are dominated by

smectite and have low gamma ray responses between 30 and 50 API. The lithological descriptor V_{shale} , generally derived for sandstones from a single log (most often gamma ray), should not, therefore, be extrapolated to mudstones.

The responses of individual logs to both grain density and TOC were also studied and were found to be weaker than the correlations between individual log response and clay content. Furthermore, there is also a difference in the log response to grain density and TOC between North Sea and Gulf of Mexico sediments. The weak correlations between a single log response and petrophysical properties generate two important conclusions: first, that it is necessary to use a multiple suite of logs to assess the petrophysical properties of mudstones; second, that to capture the complex, non-linear nature of the relationship between log responses and petrophysical properties requires the use of a mathematical approach such as that offered by ANNs.

Transformation of log data

The main aim in this work is to derive information about the solid matrix of mudstones. Since most logs are a response to both the solid matrix and the pore network, the raw log data were transformed for some logs in an attempt to remove the influence of the pore network. In all the log transformations described below, the porosity was calculated from the density log, using grain densities derived from the relevant ANN output which is described later.

m log. The *m* log is derived from the resistivity and density logs. *m* is the coefficient in the Archie equation and is dependent on rock type and texture (see Rider 1996):

$$F = \frac{1}{\phi^m} \quad (3)$$

where *F* is the formation resistivity factor and ϕ is porosity. The formation resistivity factor is defined as:

$$F = \frac{R_o}{R_w} \quad (4)$$

where R_o is the overall rock resistivity ($\text{ohm m}^2 \text{m}^{-1}$), derived from the resistivity log, and R_w is the resistivity of the formation fluid, which is assumed to be $0.1 \text{ ohm m}^2 \text{m}^{-1}$. Combining equations (3) and (4) gives the equation used to calculate *m*:

$$m = - \frac{\ln\left(\frac{R_o}{R_w}\right)}{\ln(\phi)} \quad (5)$$

D log. The *D* log is derived from the sonic and resistivity logs and is based on the work of Meyer & Nederlof (1984) who used a sonic-resistivity cross-plot to identify petroleum source rocks. Meyer & Nederlof described a parameter, *D*, which is related to transit time and resistivity as:

$$D = - 6.906 + 3.186 \log(\Delta t) + 0.487 \log(R_{75}) \quad (6)$$

where R_{75} is the resistivity at 75°F ($\text{ohms m}^2 \text{m}^{-1}$) and Δt is transit time ($\mu\text{s ft}^{-1}$). R_{75} is derived from the measured resistivity, R_t at the corresponding temperature, T (°F):

$$R_{75} = R_t \frac{T+7}{82} \quad (7)$$

Δt_m log. The Δt_m log is derived from the sonic and density logs. Δt_m is the transit time of the rock matrix and can be calculated from Wyllie *et al.*'s (1956) relationship between measured velocity and porosity. Their equation can be rearranged as:

$$\Delta t_m = \frac{\Delta t - \phi \Delta t_f}{1 - \phi} \quad (8)$$

where Δt_f is the transit time of the interstitial fluid, taken here as $200 \mu\text{s ft}^{-1}$.

ΔC log. The ΔC log, in inches, is derived from the calliper log and bit size:

$$\Delta C = \text{Calliper} - \text{bit size} \quad (9)$$

The ΔC log is included as input data to the ANNs since both mud cakes and cavings will affect log responses.

ln(b). *ln(b)* is the natural logarithmic value of burial depth and is included because depth, through compaction, affects mudstone physical properties and, thus, log responses.

TRAINING AND TESTING NETWORKS

Types of ANN models

Although there is a large training dataset from two geographically and geologically distinct locations, it was felt important to assess the ease with which the ANN approach might be extrapolated between these two locations and, perhaps, extrapolated to new locations. Therefore, one set of ANN models was constructed using only North Sea data (NS models) and a second set using a combination of both North Sea and Gulf of Mexico data (NS-GoM models). In addition, because the density log is not always available, a second set of NS-GoM models was trained in which the density log was not included as an input. There are, thus, three types of ANN models explored and used in the paper: NS models, NS-GoM models with the density log and NS-GoM models without the density log.

The inputs to the various ANN models are listed in Table 3. Inputs, which have been explained previously, are log data, transformed log data, depth and hole size. Two additional inputs require explanation. First, because there are inevitably some differences in the relationships between log response and mudstone properties in the Gulf of Mexico and North Sea, a 'location factor' has been introduced which attempts to capture these differences. Location factor can vary between zero and one and is assigned as 0.8 for North Sea samples and 0.2 for Gulf of Mexico samples. Second, the grain density determined from the appropriate ANN output is used as an input to both the TOC and clay content networks. For TOC, this reflects the fact that grain density and TOC content of mudstones are correlated. For clay content, the concern was that both gamma and sonic logs can respond in similar ways to changes in both clay content and organic content. However, the relationship between grain density and clay content is very different from that between grain density and TOC. Grain density is, thus, a useful, additional discriminant in the clay content ANNs.

In this work porosity has been estimated from the density log, not using a default grain density but rather the grain density derived from the appropriate ANN model. Because porosity is used in the calculation of the values of *m* and Δt_m (equations (5) and (8)), these transformed logs can only be used in those ANN models which include the density log as an input. For this reason the inputs to the ANNs trained without a density log are somewhat different from those trained with a density log (Table 3).

Table 3. Inputs for ANN models

ANN models	Inputs										
	GR	Resistivity	Sonic	Density	D	m	Δt_m	$\ln(b)$	ΔC	Location factor	ANN G_s
Carbonate–clastic discrimination (Models excluding density log as input)	✓	✓	✓		✓			✓	✓	✓	
Grain density	✓	✓	✓		✓			✓	✓	✓	
TOC	✓	✓	✓		✓			✓	✓	✓	✓
Clay content	✓	✓	✓		✓			✓	✓	✓	✓
Grain density (Models including density log as input)	✓	✓	✓	✓	✓			✓	✓	✓	
Carbonate–clastic discrimination	✓			✓	✓	✓	✓	✓	✓	✓	
Cementation factor	✓			✓	✓	✓	✓	✓	✓	✓	
TOC	✓			✓	✓	✓	✓	✓	✓	✓	✓
Clay content	✓			✓	✓	✓	✓	✓	✓	✓	✓

See text for explanation of D , m , Δt_m , $\ln(b)$, ΔC , location factor and ANN G_s inputs.

Training strategy

A number of strategies were used to train and test the ANNs.

- The full range of both log data and rock property data were scaled between zero and one. The rock property data were scaled between zero and one within the following ranges:
 - grain density – 2.45–2.95 g cm⁻³;
 - TOC – 0–10%;
 - clay content – 0–95%;
 - cementation factor – 0–1.
- For the carbonate–clastic discrimination models, carbonate lithologies were assigned a value of one, whilst clastic lithologies were assigned a value of zero.
- Two or three networks were trained for each petrophysical property in all three types of ANN model. Different values of α , between 0.7 and 1 (see equation (2)), were assigned to each of the 2–3 networks. A sigmoidal transfer function (equation (2)) was used to transfer data between nodes and a value of zero was always used for the constant v . Different but overlapping datasets were used to train each network, such that all the data were used in the training process. In each network, 80–90% of data were used for training and 10–20% were used for testing. The outputs from each network were then averaged to give the final prediction for each rock property. This procedure ensured that although all the data were used in the training, each network could also be tested.
- The criterion used for accepting a network was that 95% of test data should be within the error limits exhibited by 90% of the training data. Using the example of a grain density network, if 90% of the data used for training fall within the accepted error of ± 0.05 g cm⁻³, then at least 85.5% (90% \times 95%) of data used for testing must also be within this error. For example, Figure 4 compares measured clay contents with those predicted from a NS–GoM model that includes a density log input. Since the predictions for both training and test data are good, one can see that the network model trained and tested well.
- Grain density (G_s) networks were trained first. Averaged grain densities derived from the three grain density ANNs were used together with density log values to calculate porosities, which were then used in the transformation of raw log data to the transformed log data (m , Δt_m) used as inputs to other networks. The averaged grain densities were also used as inputs to the TOC and clay content networks.
- With perfect models, the output from the carbonate–clastic discrimination model would be either zero (clastic) or one (carbonate). The reality, however, is that output values can

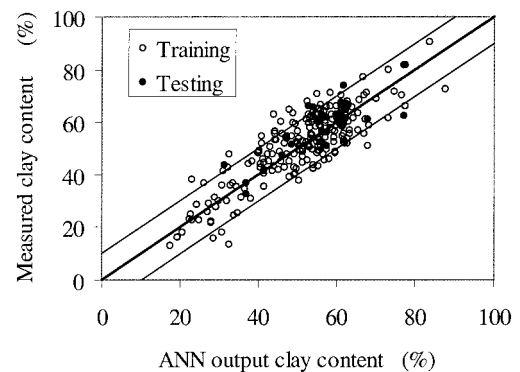


Fig. 4. Measured clay content versus clay content predicted by a NS–GoM (+density log) ANN model. The strong correlation shows that the network was not only well trained but also performed satisfactorily in the test.

vary between these two limits. A threshold value must, therefore, be chosen to discriminate fine-grained carbonates and clastics.

- Since the assignment of the value of the cementation factor is somewhat subjective, cementation factor networks were trained to a rather wide tolerance. One must accept that currently the geological information contained in the cementation factor models is imprecise and should not be used to make quantitative statements. However, it does allow the user quickly to screen sediment sections for units that have anomalous properties likely to be related to chemical and mineralogical alterations of the sediment. For example, these models might be used to explain mudstones with anomalously low porosities – for example, as a result of early diagenetic carbonate cementation.

Training results

The general performance of the trained and tested networks was investigated by running the entire North Sea and Gulf of Mexico dataset through each of the three types of network. The results are shown in Tables 1 and 2 and Figures 5–7. In general, networks that include a density log as an input perform slightly better than those without a density log. Predictions of the NS–GoM (+density log) models, for all samples, are:

- clay content: 85% of data within $\pm 10\%$ of the measured value;
- TOC: 92% of data within $\pm 1\%$ of the measured value;
- grain density: 91% of data within ± 0.07 g cm⁻³ of the measured value;

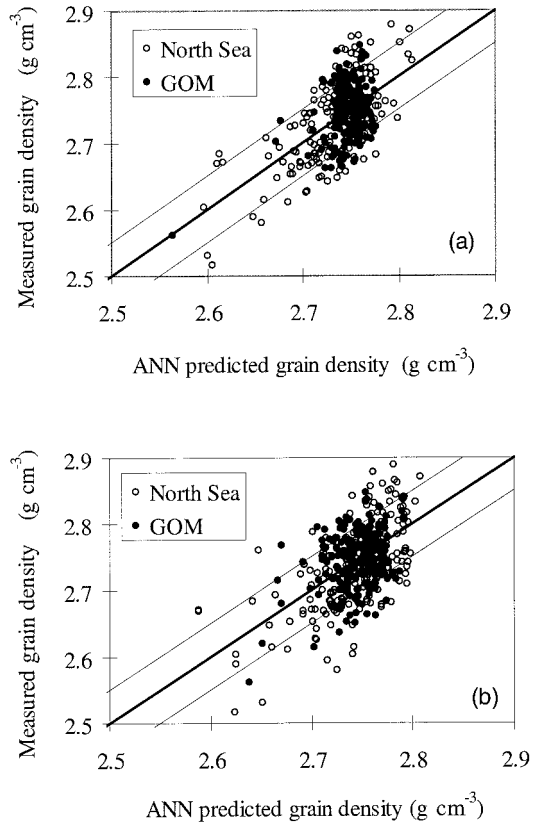


Fig. 5. Measured grain densities versus ANN-predicted grain densities: (a) NS-GoM ANNs including density log as input; (b) NS-GoM ANNs excluding density log as input.

- carbonate-clastic discrimination: 98.3% of carbonate samples and 99.9% of non-carbonate samples are classified correctly.

Global application of these techniques rests on the ability of the ANNs to generalize between locations. The results in Tables 1 and 2 and Figures 5–7 show that the NS-GoM models work equally well on both North Sea and Gulf of Mexico samples. It was also found that the predictions of the NS-GoM models on North Sea samples are very similar to those made by the NS models. In contrast, the NS models were not able to predict accurately the physical properties of Gulf of Mexico mudstones. As with any regression-based technique, there is always a question about the extent to which the results can be extrapolated, in this case to new sedimentary basins. Later, this paper will show results from West Africa which suggest that the models can work in areas away from those from where training data were supplied. Nevertheless, an initial check of ANN-predicted properties against measured data should always be taken when working in new areas.

EXAMPLES

The NS-GoM networks (with and without the density log) have been coded into a computer program: 'ShaleQuant'. ShaleQuant uses standard wireline data as input and it outputs clay content, grain density, TOC, cementation factor and the carbonate-clastic discriminant.

Examples of the output from 'ShaleQuant' are displayed in Figures 8–12 as continuous, downhole logs, along with measured data. These include data from three wells that were included in the training and testing set and two wells that were not used in training and testing the ANNs.

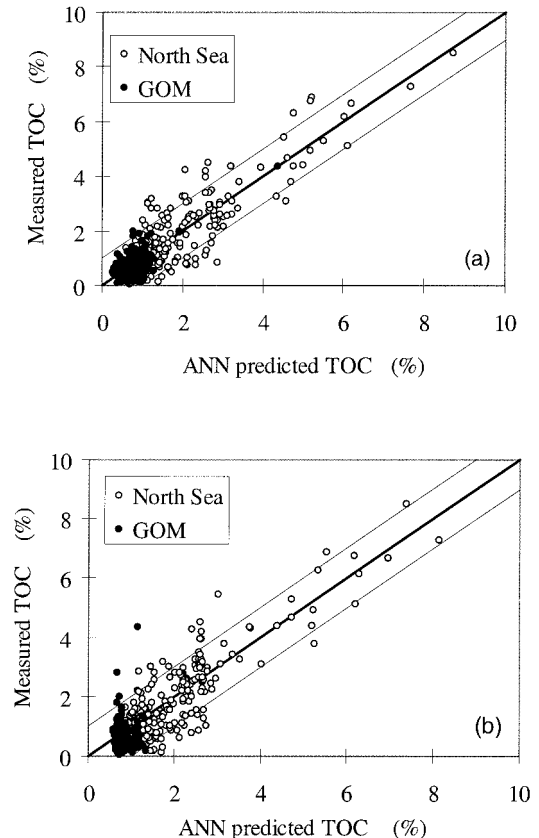


Fig. 6. Measured TOC versus ANN-predicted TOC: (a) NS-GoM ANNs including density log as input; (b) NS-GoM ANNs excluding density log as input.

Training well 1

This is the North Sea well which contains the cemented horizon (3005–3350 m) that was used to train the cementation factor networks. The generally excellent agreement between measured and predicted properties of the mudstones is shown in Figure 8. Changes in grain density, clay content and TOC are all readily observed. The cemented zone is accurately assessed between 3005 m and 3350 m and is seen to extend between 2700 m and 3600 m. Models using the density log appear to give slightly more accurate results than those which do not use the density log.

Figure 8 also illustrates some of the difficulties that emerge from the models. Above 1800 m, results are noisy, the grain densities are inaccurately modelled and, especially between 1110 m and 1320 m, there is a significant discrepancy between the outputs of the two models. Although examination of the composite log suggests that some of the 'noise' represents real lithological variability, some of the variability is due to poor log quality. The results can never be better than the quality of the log data, although one of the benefits of a multi-log approach is that problems with one log are diluted in the final output.

Because the ANNs are trained to differentiate mudstone lithologies, outputs from sand or carbonate lithologies carry no quantitative information. For sands, the ANNs generally output low clay contents, as seen in the low clay spikes in Figure 8. Better examples of sand layers can be seen in Figures 10 and 12.

Training well 2

This North Sea well contains a Cretaceous chalk section, which is accurately picked out between 800 m and 1445 m (Fig. 9). It

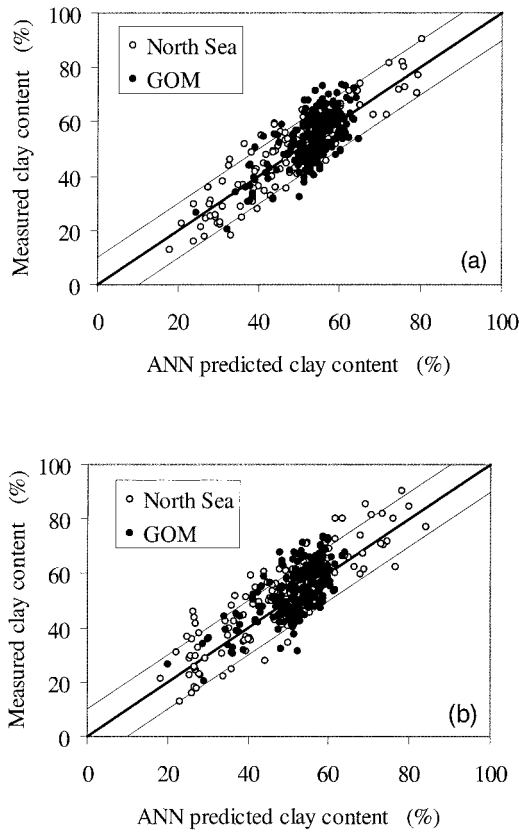


Fig. 7. Measured clay content versus ANN-predicted clay content: (a) NS–GoM ANNs including density log as input; (b) NS–GoM ANNs excluding density log as input.

also contains a 100 m thick, organic-rich Kimmeridge Clay section, which is accurately depicted around 3000 m. The change in cementation factor at 2480 m is very striking in this well, although it does not obviously relate to changes in the density and sonic logs, nor to a formation boundary. The way in which mudstones become stronger as a result of lithification or cementation, and the way in which logs respond to those changes, is an area of petrophysics that requires further investigation.

Errors resulting from the input of poor quality log data can also be seen in this well. For example, the density log around 2850 m gives values of $1.7\text{--}2.0\text{ g cm}^{-3}$, compared to values of

$2.4\text{--}2.5\text{ g cm}^{-3}$ above and below the section. Use of these data in the ANNs has resulted in predicted clay contents that are up to 20% higher than those predicted from models that did not include the density data. Quality control of log data is obviously an absolute prerequisite to the use of the ANN models.

Training well 3

Figure 10 shows the generally excellent agreement between measured and predicted properties of mudstones in a mud-dominated, deep-water Gulf of Mexico section containing a series of stacked sands. Predicted cementation factors are zero throughout, consistent with the ease with which these samples could be disaggregated using the freeze–thaw method. Since the samples in this well are sidewall cores, it is possible that discrepancies between the measured and predicted clay contents of the samples at 19 213 ft and 20 178 ft are an indication of the scale difference between the sample (centimetres) and log response (tens of centimetres). Many published photomicrographs and x-radiographs have shown the heterogeneity of mudstones on many scales (e.g. O’Brien & Slatt 1990) and our own unpublished data show that the clay content of Gulf of Mexico mudstones can vary by 20% over a few centimetres.

The sand sections in this well are clearly picked out by their predicted low clay contents and grain densities. Recall that since the ANNs were not trained using sand data, no quantitative significance can be placed on these results. This is abundantly clear for the predicted TOC contents of the section, which are accurate for the mudstones but generally very high for the sands. Furthermore, whilst the predicted TOC results from the two ANN models are similar for the sands below 19 700 ft, the two model predictions for shallower sands are different. The most likely explanation for the differing predictions is that the sands below 19 700 ft are hydrocarbon bearing.

Blind well 1

This is a North Sea well which was not used to train the ANNs. There are no outputs between 1914 m and 1945 m because no resistivity data were available. The agreement between predicted and measured properties is good and the outputs from the two models are very similar (Fig. 11). Samples from the predicted cemented zone at 1970 m contain between 1.5% and 5% inorganic carbon, supporting the prediction of a carbonate-cemented zone.

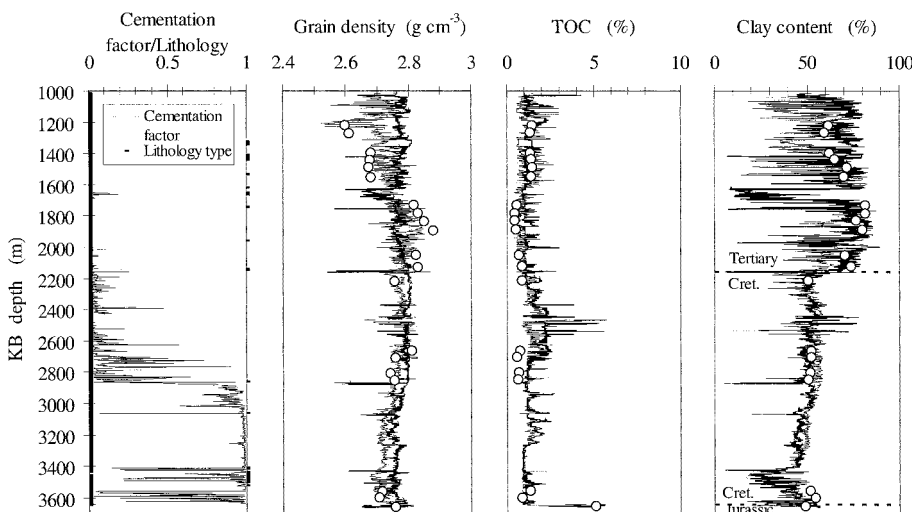


Fig. 8. Measured data for training well 1 (North Sea), with outputs from ANNs trained on both North Sea and Gulf of Mexico samples. For grain density (G_s), TOC and clay content plots, lighter lines are outputs for models trained excluding density log as an input, darker lines are outputs for models trained including density log as an input. For the lithology plot, a value of one represents carbonate, zero equals non-carbonate. Circles represent measured values. Low clay contents at 1700 m and 3640 m reflect sand/silt or carbonate layers.

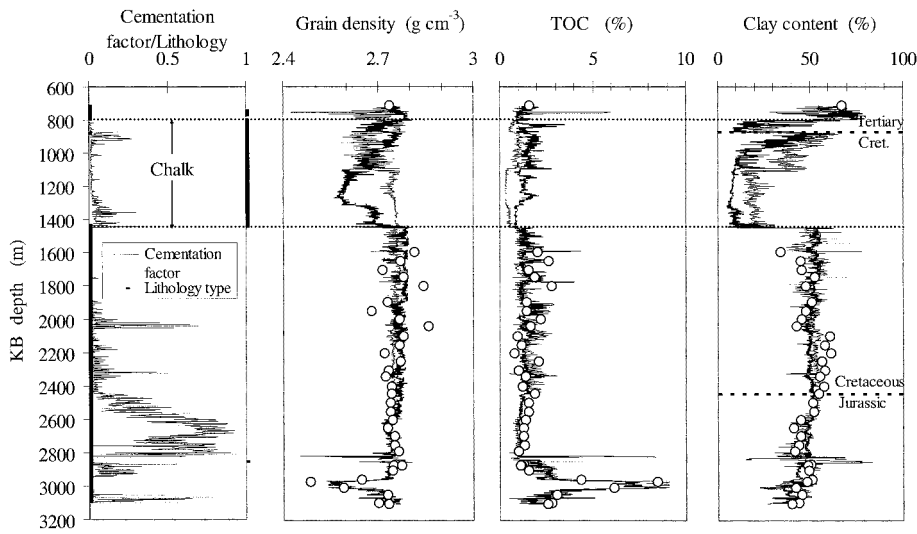


Fig. 9. Measured data for training well 2 (North Sea), with outputs from ANNs trained on both North Sea and Gulf of Mexico samples. For grain density (G_s), TOC and clay content plots, lighter lines are outputs for models trained excluding density log as an input, darker lines are outputs for models trained including density log as an input. For the lithology plot, a value of one represents carbonate, zero equals non-carbonate. Circles represent measured values. Composite log indicates that sediments around 750 m are tuff and carbonate, so that the ANN results have no significance.

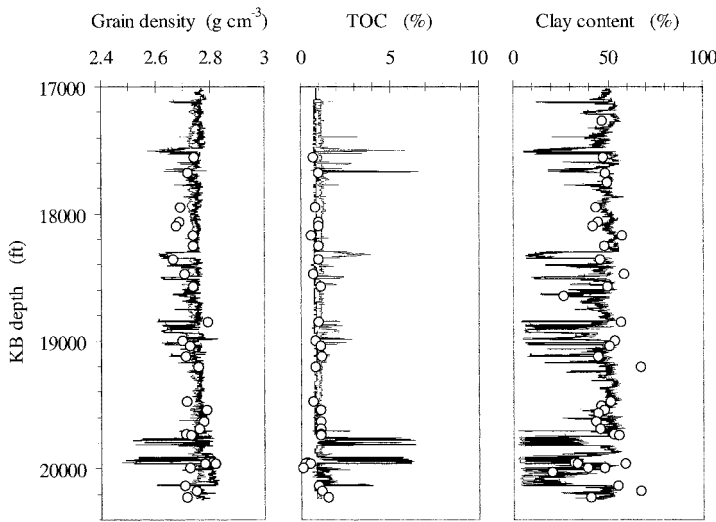


Fig. 10. Measured data for a Tertiary section in training well 3 (Gulf of Mexico), with outputs from ANNs trained on both North Sea and Gulf of Mexico samples. For grain density (G_s), TOC and clay content plots, lighter lines are outputs for models trained excluding density log as an input, darker lines are outputs for models trained including density log as an input. Circles represent measured values. Sands are denoted by spikes of low clay content, high TOC and low grain density. Data for sands have no quantitative significance.

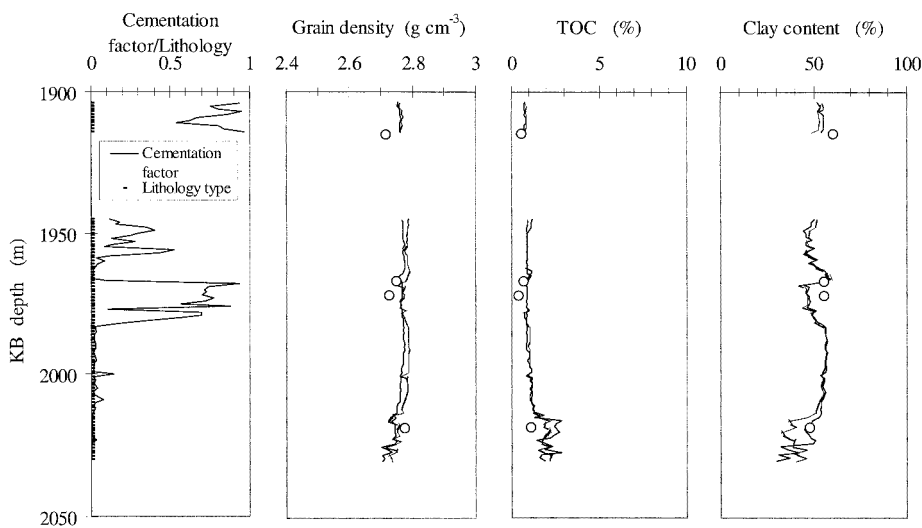


Fig. 11. Measured data for a Cretaceous section in blind well 1 (North Sea), with outputs from ANNs trained on both North Sea and Gulf of Mexico samples. For grain density (G_s), TOC and clay content plots, lighter lines are outputs for models trained excluding density log as an input, darker lines are outputs for models trained including density log as an input. Circles represent measured values.

Blind well 2

This well is from offshore West Africa and, thus, provides a test of the extent to which the ANN models can be extrapolated into regions outside those used in the training of the networks.

Use of the models in a new region requires a choice of location factor. This must be done by trial and error and means that it is important to have measured data with which to validate the use of the models. In this case, it was found that the best results were obtained using the same location factor as the North Sea,

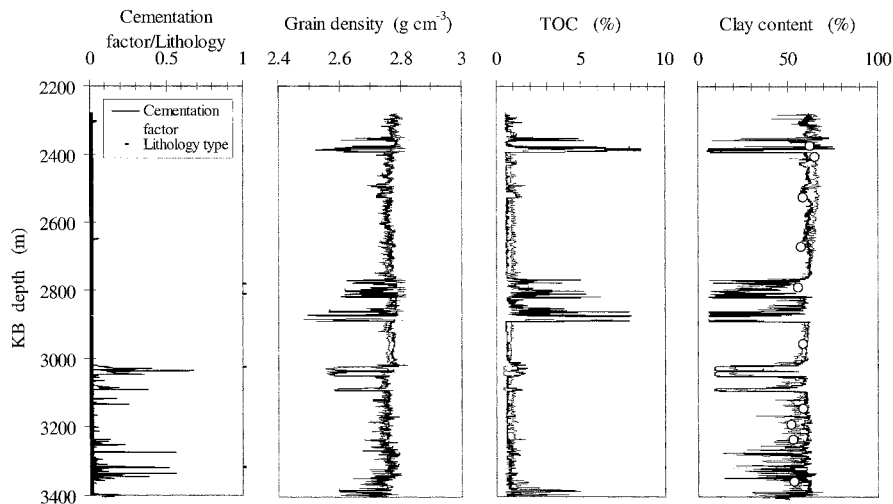


Fig. 12. Measured data for a Tertiary section in blind well 2 (West Africa), with outputs from ANNs trained on both North Sea and Gulf of Mexico samples. For grain density (G_s), TOC and clay content plots, lighter lines are outputs for models trained excluding density log as an input, darker lines are outputs for models trained including density log as an input. Circles represent measured values. Sands are denoted by spikes of low clay content, high TOC and low grain density. Data for sands have no quantitative significance. Below 3020 m, the cementation factor suggests that the sediments in some sections are moderately cemented.

implying that the log responses to the petrophysical properties of these mudstones are more similar to the North Sea than the Gulf of Mexico.

Comparison of measured data and predicted properties is shown in Figure 12. All but the two most shallow samples were cuttings and were quite heavily contaminated with oil-based drilling mud. Comparisons of measured and predicted grain densities and TOC are, thus, meaningless and are not shown in Figure 12. However, there are no source rocks in the section. Figure 12 shows that the predicted clay contents agree very well with the measured data. The mudstone sample at 2790 m is within a thick sand section. Its clay content is also accurately predicted by the ANN, but the thin unit is not easily seen on the scale used on Figure 12.

As in the Gulf of Mexico well, the sand sections in this well are indicated by anomalous predicted properties: low clay contents, low grain densities and high TOC. These results have no quantitative significance.

CONCLUDING REMARKS

This paper has shown how artificial neural networks can be used to assess rapidly and quantitatively the clay content of mudstones using commonly available wireline log data. ANNs have also been constructed to determine the grain density (and, thus, porosity), TOC and cementation factor (a measure of strength) of mudstones. It is suggested that because of the potentially complex way in which individual wireline logs respond to mudstones, the multi-log approach is an improvement on previous approaches, which use the gamma log or the combined density–neutron logs to predict the clay mineral content of mudstones.

Because the compressibility and porosity–permeability relationships of mudstones are strongly influenced by lithology, the work presented here can be used to place better constraints on the relationships between porosity, permeability and effective stress in compacting mudstone sequences. Practical applications include the evaluation of pore pressure using the porosity–effective stress relationships of mudstones, the rapid generation of the effective stress–porosity–permeability relationships, which are absolutely critical inputs to the computer-based basin models and also the evaluation of the sealing capacity of cap rocks. An ultimate aim would be to use the work outlined here to investigate the three-dimensional architecture and, thus, the fluid flow, compaction and sealing

properties of mudstone sequences, using a combined seismic–petrophysical approach.

A final point relates to what has been called here the ‘cementation factor’. This parameter was included here because it was felt that it might well relate to strength, a useful parameter when considering the mechanical properties of mudstones and important for well design and for considerations of the hydraulic consequences of fracturing (e.g. Ingram & Urai 1999). However, cementation factor remains a very poorly constrained parameter for which there is a weak understanding of related lithological properties. A sensible starting point is that cementation factor reflects the chemical diagenetic processes by which a mud is converted into a mudstone, including carbonate cementation and clay mineral diagenesis. This is an area that requires further investigation.

The work presented in this paper was supported by a NERC ROPA award, the EU FP4 and FP5 programmes, Norsk Hydro, BP and the GeoPOP consortium, comprising Amerada Hess, BG, BP, Chevron-Texaco, ConocoPhillips, ExxonMobil, JNOC, Norsk Hydro, Shell, Statoil and Total, and precursors of those companies. Norsk Hydro and BP kindly provided data and samples. The authors also thank the reviewers for their positive and thoughtful critiques

REFERENCES

- Alixant, J.-L. & Desbrandes, R. 1991. Explicit pore pressure evaluation: concept and application. *SPE Drilling Engineering*, 182–188.
- Aplin, A.C., Yang, Y.L. & Hansen, S. 1995. Assessment of β , the compression coefficient of mudstones and its relationship to detailed lithology. *Marine and Petroleum Geology*, **12**, 955–963.
- Baldwin, J.L., Bateman, R.M. & Wheatley, C.L. 1990. Application of a neural network to the problem of mineral identification from well logs. *The Log Analyst*, **31**, 279–293.
- Bethke, C.M. 1985. A numerical model of compaction driven ground water flow and heat transfer and its application to the paleohydrology of intracratonic sedimentary basins. *Journal of Geophysical Research*, **90**, 6817–6828.
- Borst, R.L. 1982. Some effects of compaction and geological time on the pore parameters of argillaceous rocks. *Sedimentology*, **29**, 291–298.
- British Standards Institution 1990. *British Standard Methods of test for Soils for civil engineering purposes, Part 2, Classification tests (BS 1377: Part 2: 1990)*. British Standard Institution, London.
- Burland, J.B. 1990. On the compressibility and shear strength of natural clays. *Géotechnique*, **40**, 329–378.
- Burrus, J. 1998. Overpressure models for clastic rocks, their relation to hydrocarbon expulsion: A critical reevaluation. In: Law, B.E., Ulmishak, G.F. & Slavin, V.I. (eds) *Abnormal Pressures in Hydrocarbon Environments*. American Association of Petroleum Geologists Memoir, **70**, 35–63.
- Dewhurst, D.N., Aplin, A.C., Sarda, J.P. & Yang, Y.L. 1998. Compaction-driven evolution of poroperm in natural mudstones: an experimental study. *Journal of Geophysical Research*, **103**(B1), 651–661.

- Dewhurst, D.N., Aplin, A.C. & Sarda, J.P. 1999a. Influence of clay fraction on pore-scale properties and hydraulic conductivity of experimentally compacted mudstones. *Journal of Geophysical Research*, **104**(B14), 29261–29274.
- Dewhurst, D.N., Yang, Y.L. & Aplin, A.C. 1999b. Permeability and fluid flow in natural mudstones. In: Aplin, A.C., Fleet, A.J. & Macquaker, J.H.S (eds) *Muds and Mudstones: Physical and Fluid-flow Properties*. Geological Society, London, Special Publications, **158**, 22–43.
- Doveton, J.H. 1994. *Geologic Log Analysis Using Computer Methods*. AAPG Computer Applications in Geology, **2**. AAPG, Tulsa.
- Gregg, S.J. & Sing, K.S.W. 1967. *Adsorption, Surface Area and Porosity*. Academic Press, New York.
- Hearst, J.R., Nelson, P.H. & Paillet, F.L. 2000. *Well logging for physical properties* (2nd edn). John Wiley & Sons, Chichester.
- Huang, Z. & Williamson, M.A. 1996. Artificial neural network modelling as an aid to source rock characterization. *Marine and Petroleum Geology*, **13**, 277–290.
- Ingram, G.M. & Urai, J.L. 1999. Top-seal leakage through faults and fractures: the role of mudrock properties. In: Aplin, A.C., Fleet, A.J. & Macquaker, J.H.S. (eds) *Muds and Mudstones: Physical and Fluid-flow Properties*. Geological Society, London, Special Publications, **158**, 125–135.
- Kaldi, J.G. & Atkinson, C.D. 1997. Evaluating seal potential: Example from the Talang Akar Formation, offshore northwest Java, Indonesia. In: Surdam, R.C. (ed.) *Seals, Traps and the Petroleum System*. American Association of Petroleum Geologists Memoir, **67**, 85–101.
- Katsube, T.J. & Williamson, M.A. 1994. Effects of diagenesis on clay nanopore structure and implications for sealing capacity. *Clay Minerals*, **29**, 451–461.
- Lerche, I. 1990. *Basin Analysis: Quantitative methods*, **1, 2**. Academic Press, San Diego, California.
- Luo, X. & Vasseur, G. 1992. Contributions of compaction and aquathermal pressure to geopressure and the influence of environmental conditions. *American Association of Petroleum Geologists Bulletin*, **76**, 1550–1559.
- Meyer, B.L. & Nederlof, M.H. 1984. Identification of source rocks wireline logs by density/resistivity and sonic transit time/resistivity crossplots. *American Association of Petroleum Geologists Bulletin*, **68**, 121–129.
- Neuzil, C.E. 1994. How permeable are clays and shales? *Water Resources Research*, **22**, 145–150.
- O'Brien, N.R. & Slatt, R.M. 1990. *Argillaceous Rock Atlas*. Springer Verlag, New York.
- Osborne, D.A. 1992. Neural networks provide more accurate reservoir permeability. *Oil & Gas Journal*, **90**, 80–83.
- Patterson, D.W. 1995. *Artificial Neural Networks: Theory and Applications*. Prentice Hall, New Jersey.
- Picard, M.D. 1971. Classification of fine-grained sedimentary rocks. *Journal of Sedimentary Petrology*, **41**, 179–195.
- Pulli, J.J. & Dysart, P.S. 1990. An experiment in the use of trained neural networks for regional seismic event classification. *Geophysical Research Letters*, **17**, 977–980.
- Rider, M.H. 1996. *The geological interpretation of well logs* (2nd edn). Whittles Publishing, Caithness.
- Rogers, S.J., Fang, J.H., Karr, C.L. & Stanley, D.A. 1992. Determination of lithology from well logs using a neural network. *American Association of Petroleum Geologists Bulletin*, **76**, 731–739.
- Rogers, S.J., Chen, H.C., Kopaska-Merkel, D.C. & Fang, J.H. 1995. Predicting permeability from porosity using artificial neural networks. *American Association of Petroleum Geologists Bulletin*, **79**, 1786–1797.
- Ross, S. & Oliver, J.P. 1964. *On Physical Adsorption*. Interscience Publishers, New York.
- Rummelhart, D.E. & McClelland, J.L. 1986. *Parallel Distributed Processing: Explorations in the Microstructure of Cognition*. MIT Press, Cambridge, MA.
- Schlömer, S. & Krooss, B.M. 1997. Experimental characterization of the hydrocarbon sealing efficiency of caprocks. *Marine and Petroleum Geology*, **14**, 565–580.
- Schmoker, J.W. 1979. Determination of organic content of Appalachian Devonian shale from formation-density logs. *American Association of Petroleum Geologists Bulletin*, **63**, 1504–1537.
- Schmoker, J.W. 1981. Determination of organic matter content of Appalachian Devonian shale from gamma-ray logs. *American Association of Petroleum Geologists Bulletin*, **65**, 1285–1298.
- Schneider, F., Burrus, J. & Wolf, S. 1993. Modelling overpressures by effective-stress/porosity relationships in low-permeability rocks: empirical artefact of physical reality? In: Doré, A.G. (ed.) *Basin Modelling: Advances and Applications*. Norwegian Petroleum Society (NPF) Special Publication, **3**. Elsevier, Amsterdam, 333–341.
- Sharp, J.M. & Domenico, A. 1976. Energy transport in thick sequences of compacting sediment. *Geological Society of America Bulletin*, **87**, 390–400.
- Skempton, A.W. 1944. Notes on the compressibility of clay. *Quarterly Journal of the Geological Society of London*, **87**, 390–400.
- Skempton, A.W. 1970. The consolidation of clays by gravitational compaction. *Quarterly Journal of the Geological Society of London*, **125**, 373–411.
- Smith, J.E. 1971. The dynamics of shale compaction and evolution of pore fluid pressure. *Mathematical geology*, **3**(3), 239–263.
- Ungerer, P., Burrus, J., Doligez, B., Chenet, J.Y. & Bessis, F. 1990. Basin evaluation by integrated two-dimensional modeling of heat transfer, fluid-flow, hydrocarbon generation and migration. *American Association of Petroleum Geologists Bulletin*, **74**, 309–355.
- Wang, L.X. 1992. A neural detector for seismic reflectivity sequences. *IEEE Transactions Neural Networks*, **3**, 338–340.
- Wu, X. & Zhou, Y. 1992. Reserve estimation using neural network techniques. *Computers and Geoscience*, **19**, 567–575.
- Wyllie, M.R.J., Gregory, A.R. & Gardener, L.W. 1956. Elastic wave velocities in heterogeneous and porous media. *Geophysics*, **21**, 41–70.
- Yang, Y.L. & Aplin, A.C. 1997. A method for the disaggregation of mudstones. *Sedimentology*, **44**, 559–562.
- Yang, Y.L. & Aplin, A.C. 1998. Influence of lithology and effective stress on the pore size distribution and modelled permeability of some mudstones from the Norwegian margin. *Marine and Petroleum Geology*, **15**, 163–175.
- Yukler, M.A., Cornford, C. & Welte, D.H. 1978. One dimensional model to simulate geomorphic, hydrodynamic and thermodynamic development of a sedimentary basin. *Geologische Rundschau*, **67**, 960–979.
- Zupan, J. & Gasteiger, J. 1993. *Neural Networks for Chemists: an Introduction*. VCH Verlagsgesellschaft, Weinheim, Federal Republic of Germany.